ACS Medicinal Chemistry Letters

pubs.acs.org/acsmedchemlett Letter

Ahp-Cyclodepsipeptide Inhibitors of Elastase: Lyngbyastatin 7 Stability, Scalable Synthesis, and Focused Library Analysis

Danmeng Luo and Hendrik Luesch*

Cite This: https://dx.doi.org/10.1021/acsmedchemlett.9b00473 Read Online

ACCESS | Metrics & More | Article Recommendations | Supporting Information

ABSTRACT: Due to the potency and selectivity of lyngbyastatin 7 in inhibiting neutrophil elastase, a serine protease involved in numerous diseases, this cyclodepsipeptide was considered as a promising lead and subjected to further developmental studies. Lyngbyastatin 7 displayed a favorable serum and microsomal stability profile. The large-scale synthesis of key building blocks was performed on gram scale with improved yields and simplified purification procedures. To tailor the complex structure, define the minimal pharmacophore, and modulate the physicochemical properties of the lead scaffold, the first pilot library of analogues was designed and synthesized for structure−activity relationship studies. We uncovered the essential role of the side chain, indicating that the minimal structural requirements for elastase inhibition extended beyond the 3-amino-6-hydroxy-2-piperidone (Ahp) and 2-aminobutenoic acid (Abu) moieties conventionally known to convey antiprotease activity and elastase selectivity, respectively. Our studies will facilitate the design and development of this class of elastase inhibitors.

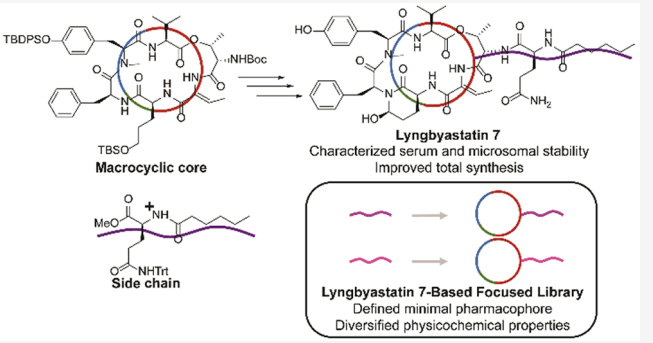

KEYWORDS: *Total synthesis, elastase inhibitor, human neutrophil elastase, macrocycle, cyclodepsipeptide*

Human neutrophil elastase (HNE, EC 3.4.21.37), a serine protease stored at high concentration in neutrophils, is known to degrade a broad spectrum of extracellular matrix (ECM) proteins, such as elastin, collagen, and fibronectin, which provide tissue physical support and stability. Under normal physiologic conditions, HNE is compartmentalized in neutrophil azurophilic granules and tightly controlled by its endogenous inhibitors, such as α1-proteinase inhibitor (α1-PI), secretory leukocyte proteinase inhibitor (SLPI), and elafin. However, at inflammation sites, the enormous release of elastase and the inactivation of endogenous inhibitors may lead to an imbalance between protease and antiprotease, which is involved in the pathogenesis of numerous diseases, such as chronic obstructive pulmonary disease (COPD), cystic fibrosis, acute lung injury (ALI), acute respiratory distress syndrome (ARDS), and pulmonary arterial hypertension (PAH).[1] Blocking the activity of elastase has been considered for a long time as a promising therapeutic strategy, and pharmaceutical companies and academic laboratories have been working for years in seeking for active small molecule elastase inhibitors to treat these life-threatening diseases.[2] However, so far only one small molecule elastase inhibitor, sivelestat sodium hydrate (ONO-5046), reached the market in Japan and South Korea, while its development in the United States and Europe was discontinued due to the fact that its clinical efficacy and safety could not be convincingly demonstrated.[3−5] In recent years, increasing evidence indicated that elastase may also play a critical role in cancer metastasis, where it could manipulate the tumor microenvironment and facilitate cancer cell migration.[6] In addition, elastase has also been linked to other inflammatory conditions, such as rheumatoid arthritis,[7,8] bowel intestinal inflammation,[9] and psoriasis.[10] Therefore, developing a novel elastase inhibitor would benefit multiple fields and has wide therapeutic applications.

As lyngbyastatin 7 (**1**),[11,12] originally isolated from a marine cyanobacterium, is one of the most potent and selective elastase inhibitors from nature, the macrocyclic depsipeptide scaffold was considered a promising starting point for developing elastase inhibitor to address the unmet medical need, complementing and contrasting other campaigns based on topologically different (flat) small molecules. The first total synthesis of lyngbyastatin 7 was recently achieved by our group utilizing a novel designed synthetic strategy (shown in Figure 1).[13] Compared with other methods to create similar molecules,[14,15] our strategy enabled easy access to lyngbyas-

Received: October 14, 2019
Accepted: February 18, 2020

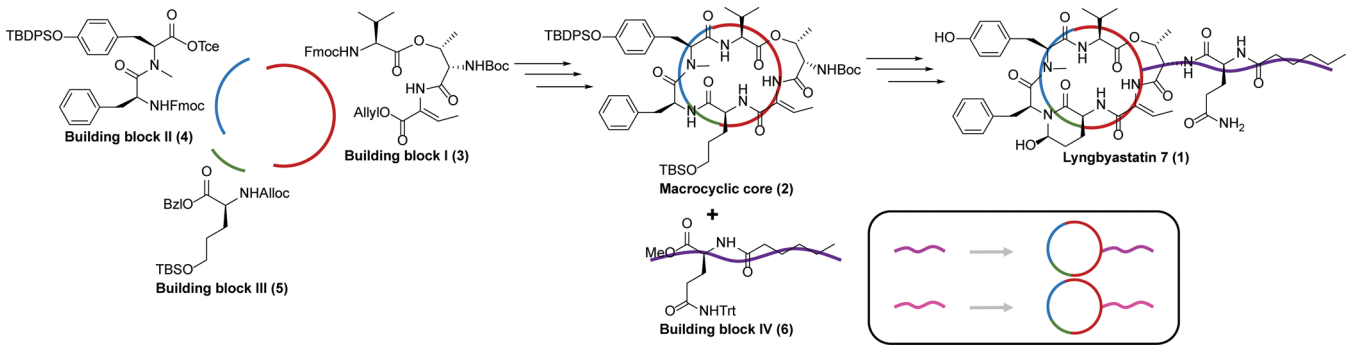

Figure 1. Synthetic strategy and key components for constructing lyngbyastatin 7 (**1**).

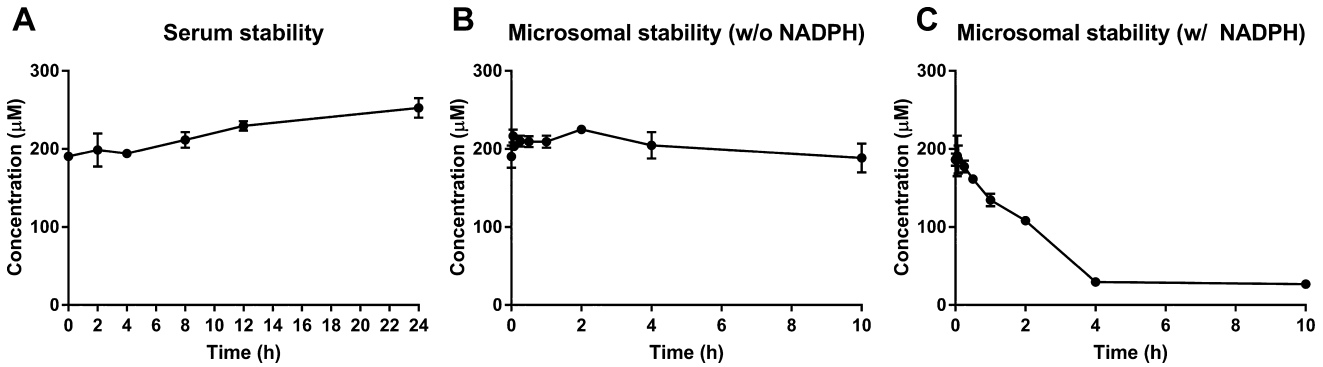

Figure 2. In vitro stability of lyngbyastatin 7 (1) under various conditions. Lyngbyastatin 7 (**1**) was incubated as indicated and extracted with EtOAc, subjected to LC-MS, and monitored by using compound-specific MRM with harmine as internal standard. (A) Stability in human serum. (B) Stability in human microsomes in the absence of NADPH. (C) Stability in human microsomes in the presence of NADPH. Data are presented as mean ± SD (n = 3).

Scheme 1. Synthesis of Building Block II (4)[a]

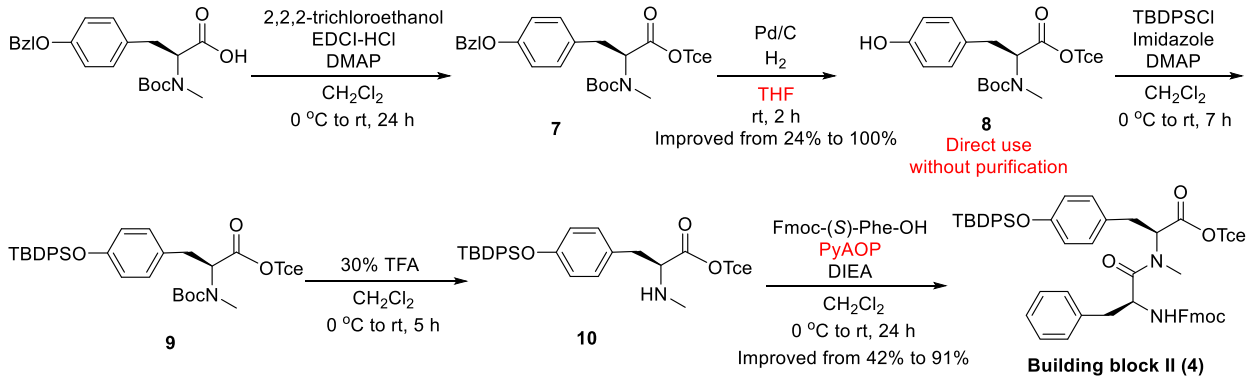

[a]Note: key optimization labeled in red.

tatin 7-based analogues with diverse side chains, as the essential macrocyclic core (**2**) was constructed first and the pendant side chain (**6**) was attached at late stage. It also facilitated the exploration of drug physicochemical property via diversifying the pendant side chain, which also paved the way for solubility optimization and formulation development.

Poor stability under physiological conditions is among the most serious but frequently occurring issues affecting therapeutic outcome. The resulting inadequate drug exposure and poor pharmacological response would not only impose the requirement of more frequent/higher daily doses (lower patient compliance and higher safety risk) but also, oftentimes, lead to the discontinuation of drug development.[16−20] Therefore, early data on the stability profile would provide in-time liability warnings and allow the removal of susceptible moieties/the blockage of metabolic sites during structural optimization.[20−24] Here, the serum and microsomal stability of lyngbyastatin 7 (**1**) was first investigated *in vitro* to provide insights into the potential stability issues inherent in (depsi)-peptide based molecules and assess the lead status of this intriguing scaffold. According to the results shown in Figure 2, lyngbyastatin 7 (**1**) was remarkably stable in human serum and remained intact over 24 h at 37 °C. Notably, the embedded amide and ester bonds proved to be resistant to hydrolysis catalyzed by serum enzymes. To evaluate the drug stability in liver, the principal site of drug metabolism, liver microsomes were incorporated here as an enzyme source, which contain the major drug-metabolizing enzymes cytochrome P450 and

https://dx.doi.org/10.1021/acsmedchemlett.9b00473
ACS Med. Chem. Lett. XXXX, XXX, XXX−XXX

Scheme 2. Synthesis of Building Block III (5)[a]

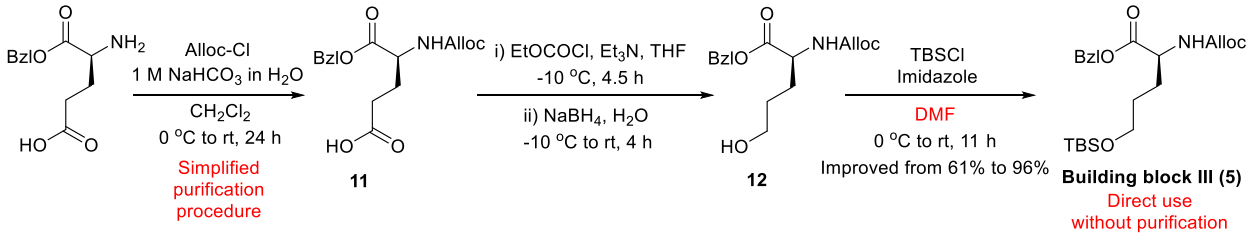

[a]Note: key optimization labeled in red.

Scheme 3. Synthesis of Macrocyclic Core (2)[a]

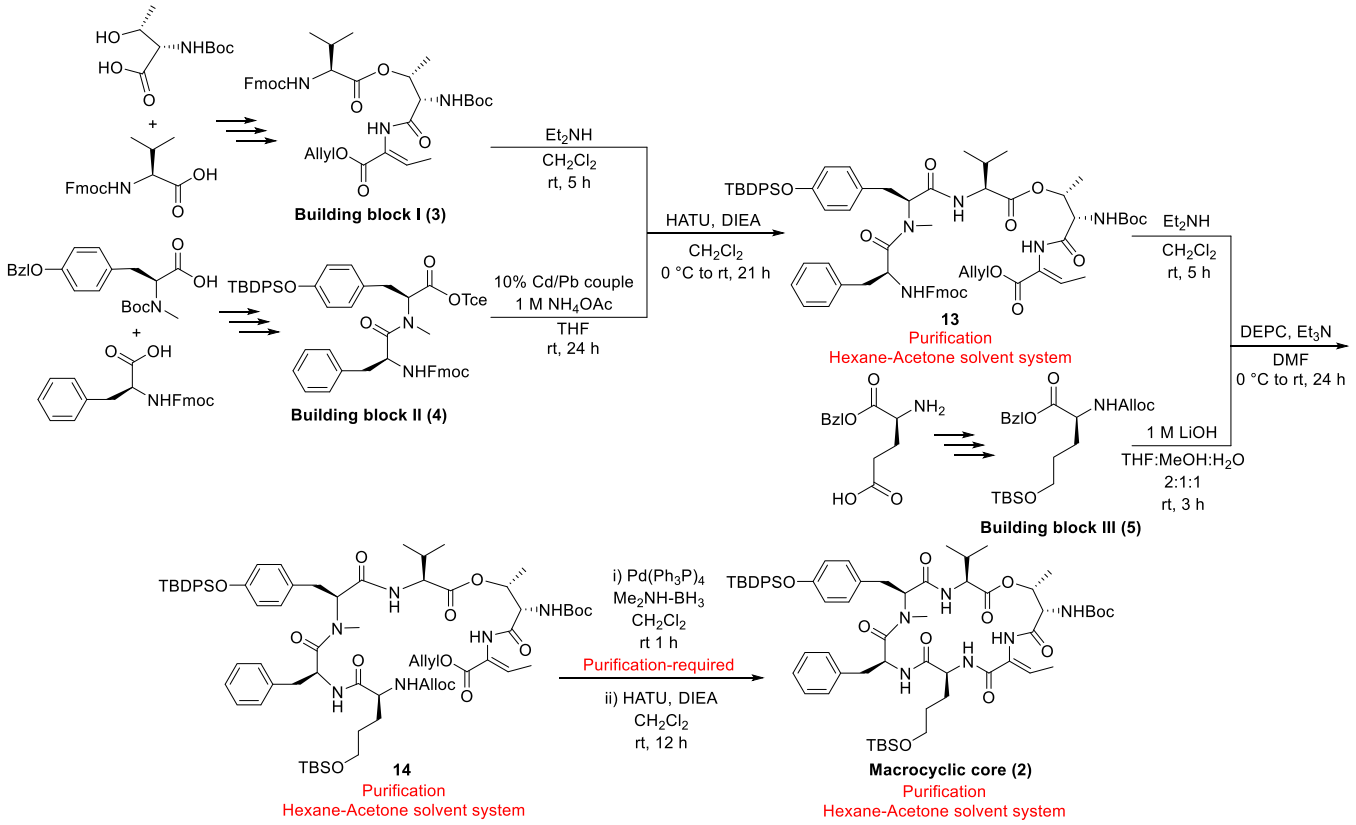

[a]Note: key optimization labeled in red.

UDP-glucuronosyltransferase. No NADPH-independent metabolism was observed when incubating lyngbyastatin 7 (**1**) with pooled human microsomes for up to 24 h. Furthermore, this compound was demonstrated to possesses a moderate microsomal metabolism rate (in the presence of NADPH cofactor) with $t_{1/2} \sim 2$ h. It is likely that the modified amino acids and the cyclized scaffold conferred good stability and resistance toward proteolytic degradation, and those features are also considered as the hallmarks of cyanobacterial metabolites, including those in preclinical development.[25−28] The excellent stability profile, especially for a depsipeptide-type molecule with such large size (molecular weight over 900 Da), strengthened the lead status for lyngbyastatin 7 (**1**) and justified further efforts.

In order to address the supply issue of lyngbyastatin 7 (**1**) and facilitate the generation of lyngbyastatin 7-based analogues, a large-scale synthesis of the key components of lyngbyastatin 7 (**1**) was performed. All the synthetic conditions in building the key components have been proven to be scalable to generate grams of materials. The four building blocks were successfully prepared in large amounts (**3** (4.9 g), **4** (51.5 g), **5** (10.2 g), and **6** (side chain, 1.6 g)), and the macrocyclic core (**2** (1.0 g)) was obtained on gram-scale. An optimized synthetic methodology for constructing the macrocycle (**2**) was developed with the aim to further improve the reaction yields and simplify the purification procedures. Here, only the steps with significant improvement are discussed.

First of all, the reaction conditions for several yield-limiting steps were optimized. For example, the step of deprotecting the benzyl group from **7** (Scheme 1) previously had a fairly low yield (24%).[13] Changing the type of catalyst or altering the dose of catalyst was ineffective in increasing the reaction yield. Through investigating potential side reactions, a transesterification product was identified, where the C-terminus Tce-ester was transformed into a methyl ester, presumably triggered by the use of methanol (MeOH) as a solvent in the reaction and workup process. By switching the solvent to tetrahydrofuran (THF) and avoiding MeOH, the yield was

https://dx.doi.org/10.1021/acsmedchemlett.9b00473
ACS Med. Chem. Lett. XXXX, XXX, XXX−XXX

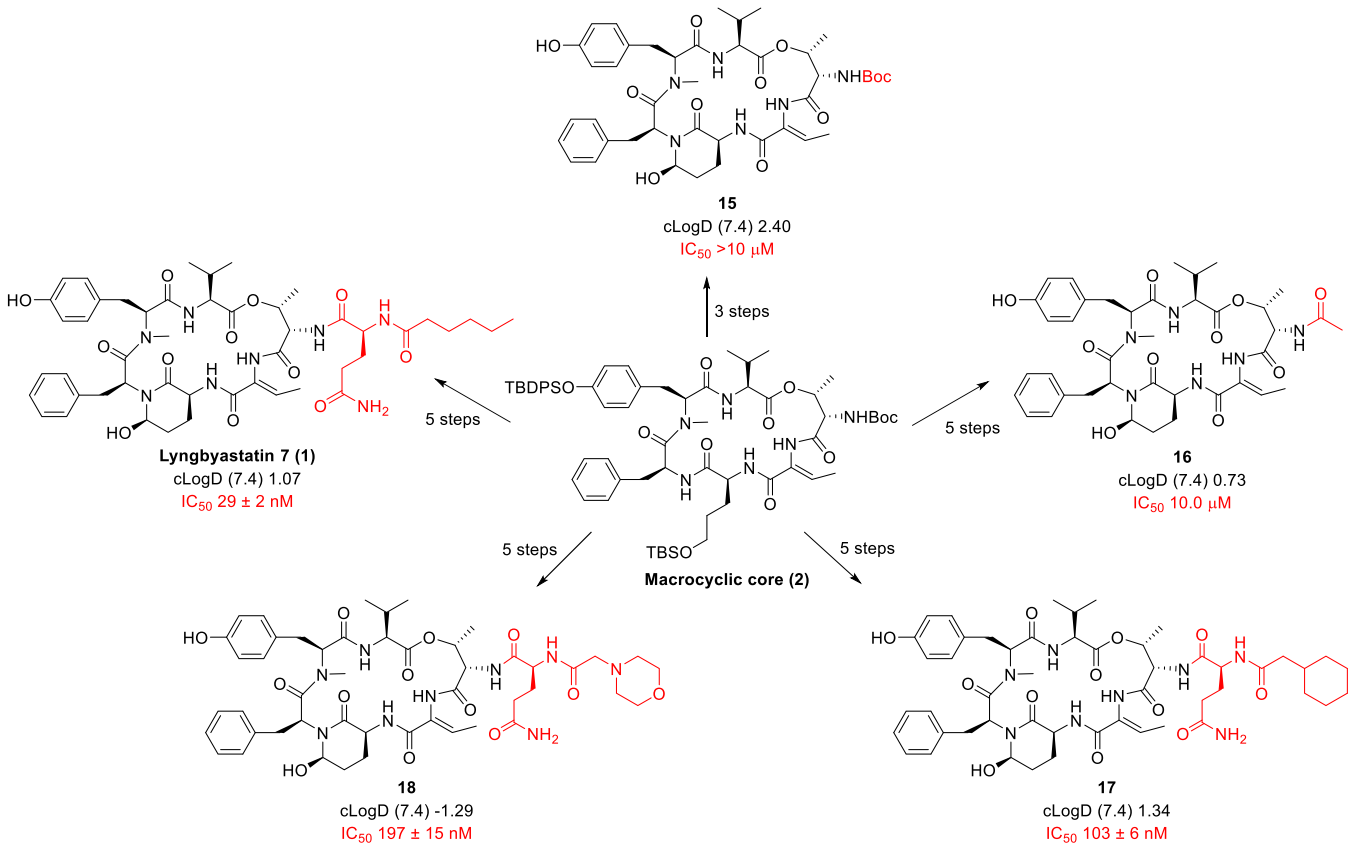

Figure 3. Structure of the essential macrocyclic core (**2**), the natural product lyngbyastatin 7 (**1**), and the synthetic analogues **15**, **16**, **17**, and **18**, as well as their corresponding cLogD values at pH 7.4 (calculated in Instant JChem) and their IC_{50} values in blocking elastase activity.

dramatically increased to approximately 100%. As for other major improvements, upon screening multiple coupling reagents, the reaction yield of synthesizing **4** (Scheme 1) was improved from 42% to 91% by using PyAOP instead of BOP-Cl. For the generation of **5** (Scheme 2), using properly dried dimethylformamide (DMF) and avoiding moisture from the environment were identified as the essential factors, which enabled the reaction yield to increase from 61% to 96%.

Second, unnecessary column chromatography steps were eliminated to simplify the purification procedures. For example, the crude product of **8** (Scheme 1), **5** (Scheme 2) and the deprotected **4** (Scheme 3) could be used directly in the next step without purification while not affecting reaction yields. In some other cases, column chromatography purification was critical to achieve a high yield for the following reaction. For instance, after removing the protecting groups from **14** (Scheme 3), a purification step was required to get rid of the remaining allyl group scavenger $Me_2NH{\cdot}BH_3$, as this reagent could react with the exposed C-terminus of this molecule and therefore interfere with the subsequent macrocyclization.

Third, a simplified purification method was developed for the step to obtain **11** (Scheme 2). Previously, column chromatography was required for this step, which was quite time-consuming as the desired product was prone to be retained on a silica gel column.[13] Taking advantage of the acidic property of this compound, a purification method using solvent-partitioning was developed. The crude reaction mixture was first basified using 10% Na_2CO_3 1,4-dioxane:H_2O 1:1 solution, followed by washing with EtOAc to remove impurities. Then the aqueous phase was acidified with 1 M HCl to pH 2−3 and extracted with EtOAc to enrich the desired product back into the organic phase. After evaporating in vacuo, the product was pure enough for use in the next reaction. Furthermore, for the purification of **13**, **14**, and **2** (Scheme 3), the hexane−acetone solvent system more efficiently separated the desired product from other potential impurities than the previously reported hexane−EtOAc system.[13]

With large amounts of the macrocyclic core (**2**) in hand, the construction of a focused library of lyngbyastatin 7-based analogues could be initiated. With the aim to trim off the complex structure, minimize the molecular weight, and investigate the role of the macrocyclic core as the sole factor in affording elastase inhibitory activity, two simplified versions of lyngbyastatin 7 were synthesized. Taking advantage of the attached *tert*-butoxycarbonyl (Boc) group, which originally served as the protecting group of the Thr amine, analogue **15** (Figure 3) was first designed and the synthesis could be easily performed within just 3 steps. In order to mimic an amide-liked short side chain, an acetyl group replaced the Boc group to afford analogue **16** (Figure 3) smoothly via 5 steps.

Solubility issues (involving approximately 75% of drug candidates currently under development) adversely affect preclinical/clinical studies.[29,30] Poor aqueous solubility would not only lead to erratic assay results (artificially weak potency, flawed good selectivity, faulty clean off-target activities, etc.) but also negatively affect the pharmacokinetic profile of the molecules of interest. In addition, drug physicochemical property is also known to be a key to develop formulations for pulmonary targeted delivery. Therefore, the key consideration in designing analogues is to differentiate their

https://dx.doi.org/10.1021/acsmedchemlett.9b00473
ACS Med. Chem. Lett. XXXX, XXX, XXX−XXX

physicochemical property. Several lyngbyastatin 7-based analogues were designed by changing the length of the terminal lipid chain, replacing the side chain amide of Gln with other polar functional groups, and attaching hydrophilicity/lipophilicity-modulating groups at the terminus of the pendant side chain. Molecular docking using Autodock Vina[31] was applied to virtually evaluate the interaction between the designed analogues and the HNE binding site (Figure S1), using the cocrystal structure of lyngbyastatin 7 and porcine pancreatic elastase (PPE)[12] as a starting point and to validate the docking approach. Several hits with improved affinity were obtained, and we first selected two analogues to corroborate our strategy to attach various side chain at late stage and to generate diverse analogues in a few steps. In addition to binding affinity of the designed molecules, we also took their cLogD into account to probe the nature of the HNE binding pocket. Moreover, if this molecule were to be developed for inhalation, hydrophilicity/lipophilicity would also affect the absorption rate and bioavailability.[32] Therefore, analogues **17** and **18** characterized by a cyclohexyl and morpholine group, respectively (Figures 3), were prioritized for synthesis due to their differential molecular properties. The synthetic strategy to generate these two molecules was similar to the previously reported one for obtaining lyngbyastatin 7 (**1**) (see Supporting Information for details).[13]

The HNE inhibitory activities of **15**, **16**, **17**, and **18** were evaluated in parallel with lyngbyastatin 7 (**1**) at the enzyme level (see Figure 3 for IC_{50} values and dose−response curves in Figure 4A for the most active compounds), and some critical information could be obtained from the structure−activity relationship (SAR) analysis. The first important message is that the side chain is actually essential to afford the elastase inhibitory activity. As the side chain was shortened to an acetyl group (compound **16**), the activity decreased over 300-fold. It is the first time that the minimal cyclodepsipeptide structure of effective elastase inhibition was defined. Although 3-amino-6-hydroxy-2-piperidone (Ahp) was the known pharmacophore and the macrocyclic conformation was known to be essential, the macrocycle alone (in acetylated form) was insufficient to substantially inhibit the enzyme. At least a minimal side chain was required to achieve recognition and binding toward HNE. Second, the elastase binding pocket could not tolerate a bulky functional group, especially at the conjunction site of the side chain and the macrocycle. As the side chain was switched to a Boc group (compound **15**), the activity was completely lost; according to the result derived from molecular docking, this structure also displayed a decreased binding affinity to HNE (−6.7 kcal/mol) compared with lyngbyastatin 7 (−7.2 kcal/mol). When bulky groups were attached at the terminal site (compounds **17** and **18**), the potency only decreased slightly. The next message is, the HNE binding pocket prefers a more lipophilic terminal chain, as the analogue with higher lipophilicity (compound **17**) retained more activity than the one with lower lipophilicity (compound **18**). It was previously known that the Abu unit adjacent to Ahp contributes to the selectivity for elastase.[6,11,12,33,34]

In addition, the potency of **17** and **18** was further assessed at the cellular and transcriptional level side by side with lyngbyastatin 7 (**1**) (Figures 4B and 4C). Compared with **1**, **17** displayed similar potency in protecting bronchial epithelial cells against elastase-induced antiproliferation, as measured by MTT assay, and in upregulating transcript levels of pro-inflammatory cytokine *IL1B*, as measured by reverse tran-

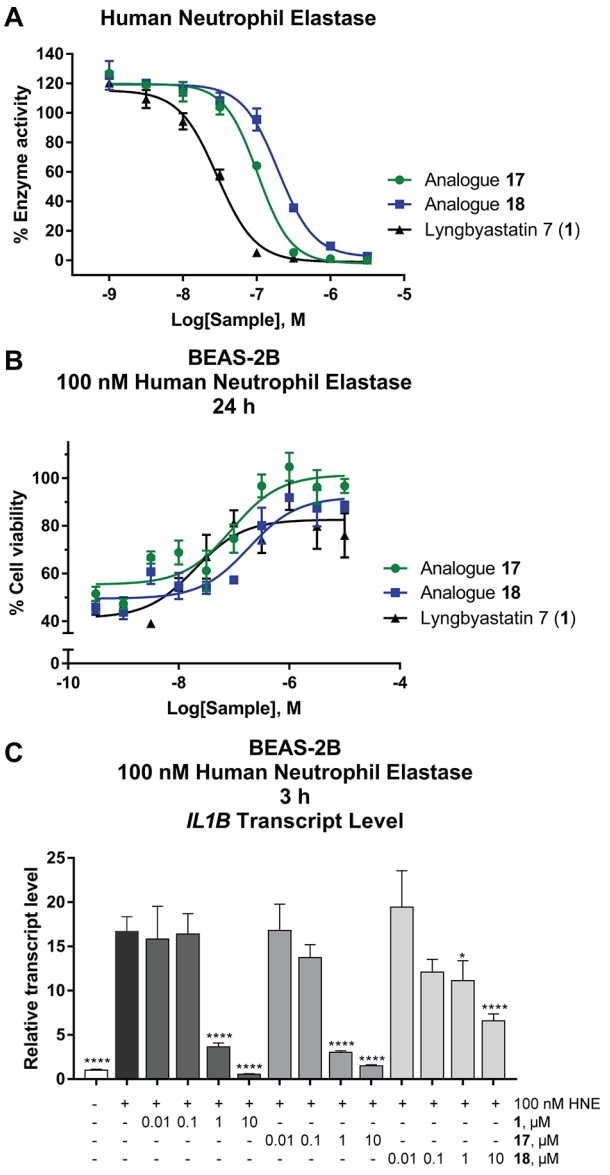

Figure 4. *In vitro* biological evaluation of lyngbyastatin 7 (**1**), analogue **17**, and analogue **18**. (A) In the HNE enzyme assay, HNE was first incubated with lyngbyastatin 7 (**1**), analogue **17**, or analogue **18**, respectively, for 15 min in 0.1 M Tris−0.5 M NaCl (pH 7.5), and then *N*-(OMe-succinyl)-Ala-Ala-Pro-Val-*p*-nitroanilide was used as substrate to monitor the enzyme activity. The IC_{50} value for each compound is 29 ± 2, 103 ± 6, and 197 ± 15 nM, respectively. Data are presented as mean ± SD (n = 3), relative to 0.5% DMSO treatment + vehicle. (B) In the cell viability assay, BEAS-2B cells were cotreated with the tested compound and 100 nM HNE for 24 h. Cell viability was monitored using MTT reagent. The EC_{50} values for lyngbyastatin 7 (**1**), analogue **17**, and analogue **18** were determined as 20 ± 4, 91 ± 17, and 185 ± 33 nM, respectively. Data are presented as mean ± SD (n = 3), relative to 0.5% DMSO treatment + vehicle. (C) In order to monitor the changes in transcript level of *IL1B* in the presence of different compounds at various concentrations, total RNA was extracted after BEAS-2B cells were cotreated with lyngbyastatin 7 (**1**), analogue **17** and analogue **18** or solvent control and 100 nM HNE or vehicle for 3 h. After cDNA synthesis, qPCR was carried out while using *GAPDH* as endogenous control. Data are presented as mean ± SD, *P < 0.05, ****P < 0.0001 compared to HNE-treated cells using ANOVA, Dunnett's t test (n = 3).

https://dx.doi.org/10.1021/acsmedchemlett.9b00473
ACS Med. Chem. Lett. XXXX, XXX, XXX−XXX

scription and quantitative polymerase chain reaction (RT-qPCR), while **18** was less effective. Their performance is in agreement with the trend observed at the enzyme level (Figure 4A).

In conclusion, an optimized and scalable synthetic methodology was developed for large-scale synthesis of all the key components of lyngbyastatin 7 (**1**) with improved reaction yields and simplified purification procedures. All four building blocks were obtained in large amounts and the critical macrocyclic core was smoothly obtained on gram-scale. To translate natural products into pharmacotherapeutics, it is also critical to take the stability issue into concern at early stage to avoid costly and risky development. Lyngbyastatin 7 was shown to be stable in serum and possess a reasonable microsomal metabolic rate, which further highlighted its drug-likeness and reaffirmed its lead status. A pilot library of lyngbyastatin 7 (**1**) analogues was constructed to tailor the molecules and modulate the lipophilicity/hydrophilicity through pendant side chain manipulation. For the first time synthetic analogues were easily accessed within 3−5 steps from a common key intermediate, validating the design of our synthetic strategy, which enabled the attachment of the side chain at late stage and provides opportunities for straightforward diversification. Moreover, equipped with the improved understanding of the HNE binding pocket deduced via SAR study, the molecular design of lyngbyastatin 7-based analogues could be navigated in a more precise manner in the future. In addition, the entry to three active molecules with different lipophilicity/hydrophilicity also provides the opportunity to develop formulations for different routes of administration for pulmonary delivered therapeutics or for other disease indications with overactive HNE.

■ ASSOCIATED CONTENT

Supporting Information

The Supporting Information is available free of charge at https://pubs.acs.org/doi/10.1021/acsmedchemlett.9b00473.

Experimental details, supplementary results and discussion of molecular docking, Figure S1, and NMR spectra for synthetic compounds (PDF)

■ AUTHOR INFORMATION

Corresponding Author

Hendrik Luesch − *Department of Medicinal Chemistry and Center for Natural Products, Drug Discovery and Development (CNPD3), University of Florida, Gainesville, Florida 32610, United States*; orcid.org/0000-0002-4091-7492; Phone: +1-352-273-7738; Email: luesch@cop.ufl.edu; Fax: +1-352-273-7741

Author

Danmeng Luo − *Department of Medicinal Chemistry and Center for Natural Products, Drug Discovery and Development (CNPD3), University of Florida, Gainesville, Florida 32610, United States*

Complete contact information is available at: https://pubs.acs.org/10.1021/acsmedchemlett.9b00473

Author Contributions

The manuscript was written through contributions of all authors. All authors have given approval to the final version of the manuscript.

Funding

This research was supported by the UF College of Pharmacy PROSPER grant and the National Institutes of Health grant R01CA172310.

Notes

The authors declare no competing financial interest.

■ ACKNOWLEDGMENTS

We thank J. Rocca (Advanced Magnetic Resonance Imaging and Spectroscopy) for assistance with NMR data acquisition.

■ ABBREVIATIONS

BOP-Cl bis(2-oxo-3-oxazolidinyl)phosphinic chloride
DEPC diethyl phosphorocyanidate
DIEA *N*,*N*-diisopropylethylamine
DMAP 4-(dimethylamino)pyridine
EDCI·HCl *N*-ethyl-*N*′-(3-(dimethylamino)propyl) carbodiimide hydrochloride
HATU 1-[bis(dimethylamino)methylene]-1*H*-1,2,3-triazolo[4,5-*b*]pyridinium 3-oxide hexafluorophosphate
MTT 3-(4,5-dimethylthiazol-2-yl)-2,5-diphenyltetrazolium bromide
NADPH nicotinamide adenine dinucleotide phosphate
PyAOP (7-azabenzotriazol-1-yloxy)-trispyrrolidinophosphonium hexafluorophosphate
TBDPS *tert*-butyldiphenylsilyl
TBS *tert*-butyldimethylsilyl
Tce trichloroethyl
Trt triphenylmethyl
UDP uridine diphosphate

■ REFERENCES

(1) Korkmaz, B.; Horwitz, M. S.; Jenne, D. E.; Gauthier, F. Neutrophil Elastase, Proteinase 3, and Cathepsin G as Therapeutic Targets in Human Diseases. *Pharmacol. Rev.* **2010**, *62*, 726−759.

(2) Crocetti, L.; Quinn, M. T.; Schepetkin, I. A.; Giovannoni, M. P. A Patenting Perspective on Human Neutrophil Elastase (HNE) Inhibitors (2014−2018) and Their Therapeutic Applications. *Expert Opin. Ther. Pat.* **2019**, *29*, 1−24.

(3) Kawabata, K.; Suzuki, M.; Sugitani, M.; Imaki, K.; Toda, S.; Miyamoto, T. ONO-5046, a Novel Inhibitor of Human Neutrophil Elastase. *Biochem. Biophys. Res. Commun.* **1991**, *177*, 814−820.

(4) Iwata, K.; Doi, A.; Ohji, G.; Oka, H.; Oba, Y.; Takimoto, K.; Igarashi, W.; Gremillion, D. H.; Shimada, T. Effect of Neutrophil Elastase Inhibitor (Sivelestat Sodium) in the Treatment of Acute Lung Injury (ALI) and Acute Respiratory Distress Syndrome (ARDS): A Systematic Review and Meta-Analysis. *Intern. Med.* **2010**, *49*, 2423−2432.

(5) Aikawa, N.; Ishizaka, A.; Hirasawa, H.; Shimazaki, S.; Yamamoto, Y.; Sugimoto, H.; Shinozaki, M.; Taenaka, N.; Endo, S.; Ikeda, T.; Kawasaki, Y. Reevaluation of the Efficacy and Safety of the Neutrophil Elastase Inhibitor, Sivelestat, for the Treatment of Acute Lung Injury Associated with Systemic Inflammatory Response Syndrome; a Phase IV Study. *Pulm. Pharmacol. Ther.* **2011**, *24*, 549−554.

(6) Al-Awadhi, F. H.; Paul, V. J.; Luesch, H. Structural Diversity and Anticancer Activity of Marine-Derived Elastase Inhibitors: Key Features and Mechanisms Mediating the Antimetastatic Effects in Invasive Breast Cancer. *ChemBioChem* **2018**, *19*, 815−825.

(7) Cawston, T. E.; Young, D. A. Proteinases Involved in Matrix Turnover during Cartilage and Bone Breakdown. *Cell Tissue Res.* **2010**, *339*, 221−235.

(8) Di Cesare Mannelli, L.; Micheli, L.; Cinci, L.; Maresca, M.; Vergelli, C.; Pacini, A.; Quinn, M. T.; Paola Giovannoni, M.; Ghelardini, C. Effects of the Neutrophil Elastase Inhibitor EL-17 in Rat Adjuvant-Induced Arthritis. *Rheumatology* **2016**, *55*, 1285−1294.

(9) Langhorst, J.; Elsenbruch, S.; Koelzer, J.; Rueffer, A.; Michalsen, A.; Dobos, G. J. Noninvasive Markers in the Assessment of Intestinal Inflammation in Inflammatory Bowel Diseases: Performance of Fecal Lactoferrin, Calprotectin, and PMN-Elastase, CRP, and Clinical Indices. *Am. J. Gastroenterol.* **2008**, *103*, 162−169.
(10) Wiedow, O.; Wiese, F.; Streit, V.; Kalm, C. Lesional Elastase Activity in Psoriasis, Contact Dermatitis, and Atopic Dermatitis. *J. Invest. Dermatol.* **1992**, *99*, 306−309.
(11) Taori, K.; Matthew, S.; Rocca, J. R.; Paul, V. J.; Luesch, H. Lyngbyastatins 5−7, Potent Elastase Inhibitors from Floridian Marine Cyanobacteria, *Lyngbya spp*. *J. Nat. Prod.* **2007**, *70*, 1593−1600.
(12) Salvador, L. A.; Taori, K.; Biggs, J. S.; Jakoncic, J.; Ostrov, D. A.; Paul, V. J.; Luesch, H. Potent Elastase Inhibitors from Cyanobacteria: Structural Basis and Mechanisms Mediating Cytoprotective and Anti-Inflammatory Effects in Bronchial Epithelial Cells. *J. Med. Chem.* **2013**, *56*, 1276−1290.
(13) Luo, D.; Chen, Q.-Y.; Luesch, H. Total Synthesis of the Potent Marine-Derived Elastase Inhibitor Lyngbyastatin 7 and in Vitro Biological Evaluation in Model Systems for Pulmonary Diseases. *J. Org. Chem.* **2016**, *81*, 532−544.
(14) Yokokawa, F.; Shioiri, T. Total Synthesis of Somamide A, an Ahp (3-Amino-6-Hydroxy-2-Piperidone)-Containing Cyclic Depsipeptide. *Tetrahedron Lett.* **2002**, *43*, 8673−8677.
(15) Kocher, S.; Rey, J.; Bongard, J.; Tiaden, A. Ø. N.; Meltzer, M.; Richards, P. J.; Ehrmann, M.; Kaiser, M. Chemical Probes Tailored Ahp-Cyclodepsipeptides as Potent Non-Covalent Serine Protease Inhibitors. *Angew. Chem., Int. Ed.* **2017**, *56*, 8555−8558.
(16) Nicolaou, K. C. Advancing the Drug Discovery and Development Process. *Angew. Chem.* **2014**, *126*, 9280−9292.
(17) Bleicher, K. H.; Böhm, H. J.; Müller, K.; Alanine, A. I. Hit and Lead Generation: Beyond High-Throughput Screening. *Nat. Rev. Drug Discovery* **2003**, *2*, 369−378.
(18) Waring, M. J.; Arrowsmith, J.; Leach, A. R.; Leeson, P. D.; Mandrell, S.; Owen, R. M.; Pairaudeau, G.; Pennie, W. D.; Pickett, S. D.; Wang, J.; Wallace, O.; Weir, A. An Analysis of the Attrition of Drug Candidates from Four Major Pharmaceutical Companies. *Nat. Rev. Drug Discovery* **2015**, *14*, 475−486.
(19) Kola, I.; Landis, J. Can the Pharmaceutical Industry Reduce Attrition Rates? *Nat. Rev. Drug Discovery* **2004**, *3*, 1−5.
(20) *Drug-like Properties: Concepts, Structure Design and Methods: From ADME to Toxicity Optimization*; Kerns, E. H., Di, L., Eds.; Elsevier Inc., 2008.
(21) Chen, J.; Li, W.; Yao, H.; Xu, J. Insights into Drug Discovery from Natural Products through Structural Modification. *Fitoterapia* **2015**, *103*, 231−241.
(22) Masimirembwa, C. M.; Bredberg, Ui.; Andersson, T. B. Metabolic Stability for Drug Discovery and Development: Pharmacokinetic and Biochemical Challenges. *Clin. Pharmacokinet.* **2003**, *42*, 515−528.
(23) Thompson, T. N. Optimization of Metabolic Stability as a Goal of Modern Drug Design. *Med. Res. Rev.* **2001**, *21*, 412−449.
(24) Di, L.; Kerns, E. H.; Hong, Y.; Chen, H. Development and Application of High Throughput Plasma Stability Assay for Drug Discovery. *Int. J. Pharm.* **2005**, *297*, 110−119.
(25) Hong, J.; Luesch, H. Largazole: From Discovery to Broad-Spectrum Therapy. *Nat. Prod. Rep.* **2012**, *29*, 449−456.
(26) Cai, W.; Ratnayake, R.; Gerber, M. H.; Chen, Q.; Yu, Y.; Derendorf, H.; Trevino, J. G.; Luesch, H. Development of Apratoxin S10 (Apra S10) as an Anti-Pancreatic Cancer Agent and Its Preliminary Evaluation in an Orthotopic Patient-Derived Xenograft (PDX) Model. *Invest. New Drugs* **2019**, *37*, 364−374.
(27) Naylor, M. R.; Bockus, A. T.; Blanco, M.; Lokey, R. S. Cyclic Peptide Natural Products Chart the Frontier of Oral Bioavailability in the Pursuit of Undruggable Targets. *Curr. Opin. Chem. Biol.* **2017**, *38*, 141−147.
(28) Blanco, M. *Cyclic Peptide Design*; Goetz, G., Ed.; Humana Press, 2019.
(29) Williams, H. D.; Trevaskis, N. L.; Charman, S. A.; Shanker, R. M.; Charman, W. N.; Pouton, C. W.; Porter, C. J. H. Strategies to Address Low Drug Solubility in Discovery and Development. *Pharmacol. Rev.* **2013**, *65*, 315−499.
(30) Di, L.; Fish, P. V.; Mano, T. Bridging Solubility between Drug Discovery and Development. *Drug Discovery Today* **2012**, *17*, 486−495.
(31) Trott, O.; Olson, A. J. Software News and Update AutoDock Vina: Improving the Speed and Accuracy of Docking with a New Scoring Function, Efficient Optimization, and Multithreading. *J. Comput. Chem.* **2009**, *31*, 455−461.
(32) Patton, J. S.; Fishburn, C. S.; Weers, J. G. The Lungs as a Portal of Entry for Systemic Drug Delivery. *Proc. Am. Thorac. Soc.* **2004**, *1*, 338−344.
(33) Nagarajan, M.; Maruthanayagam, V.; Sundararaman, M. SAR Analysis and Bioactive Potentials of Freshwater and Terrestrial Cyanobacterial Compounds: A Review. *J. Appl. Toxicol.* **2013**, *33*, 313−349.
(34) Resch, S.; Kessenbrock, T.; Schrapp, L.; Ehrmann, M.; Kaiser, M. From Dolastatin 13 to Cyanopeptolins, Micropeptins, and Lyngbyastatins: The Chemical Biology of Ahp-Cyclodepsipeptides. *Nat. Prod. Rep.* **2020**, *37*, 163−174.

https://dx.doi.org/10.1021/acsmedchemlett.9b00473
ACS Med. Chem. Lett. XXXX, XXX, XXX−XXX